AD_____

Award Number: W81XWH-09-1-0009

TITLE: Characterization of Physiological Roles and Prognostic Importance of IR/IGF-IR Hybrid Receptors in Breast Cancer

PRINCIPAL INVESTIGATOR: Yu-Fen Wang, B.S.

CONTRACTING ORGANIZATION: Baylor College of Medicine, Houston, TX, 77030

REPORT DATE: January 2011

TYPE OF REPORT: Annual Summary

PREPARED FOR: U.S. Army Medical Research and Materiel Command
Fort Detrick, Maryland 21702-5012

DISTRIBUTION STATEMENT:

√ Approved for public release; distribution unlimited

REPORT DOCUMENTATION PAGE

Form Approved
OMB No. 0704-0188

1. REPORT DATE *(DD-MM-YYYY)*	**2. REPORT TYPE**	**3. DATES COVERED** *(From - To)*
01-01-2011	Annual Summary	15 DEC 2009 - 14 DEC 2010

4. TITLE AND SUBTITLE
Characterization of Physiological Roles and Prognostic

of IR/IGF-IR Hybrid Receptors in Breast Cancer

5a. CONTRACT NUMBER

5b. GRANT NUMBER
W81XWH-09-1-0009

5c. PROGRAM ELEMENT NUMBER

6. AUTHOR(S)
Yu-Fen Wang, B.S.

5d. PROJECT NUMBER

5e. TASK NUMBER

5f. WORK UNIT NUMBER

7. PERFORMING ORGANIZATION NAME(S) AND ADDRESS(ES)
Baylor College of Medicine,
Houston, TX, 77030

8. PERFORMING ORGANIZATION REPORT

9. SPONSORING / MONITORING AGENCY NAME(S) AND ADDRESS(ES)

U.S. Army Medical Research and Materiel
Fort Detrick, Maryland 21702-5012

10. SPONSOR/MONITOR'S ACRONYM(S)

11. SPONSOR/MONITOR'S REPORT NUMBER(S)

12. DISTRIBUTION / AVAILABILITY STATEMENT
Approved for public release; distribution unlimited

13. SUPPLEMENTARY NOTES

14. ABSTRACT

An inducible dimerization system will be used to study the IR/IGF-IR Hybrid receptor by constructing chimeric IR and chimeric IGF-IR with different dimerization domains. Chimeric IR and chimeric IGFIR retroviral vectors for homo and heterodimeriation were generated. Stable MCF10A clones expressing only chimeric IR or chimeric IGF-IR allowing homodimerization were established. Homodimerizer AP20187 treatment was able to induce activation of chimeric IGF-IR and chimeric IR in a dose dependant manner and was able to activate AKT and ERK pathways. However, I have encounter technical difficulties in establishing cells expressing both chimeric IR and chimeric IGF-IR. To measure the IR/IGF-IR hybrid receptor on paraffin embedded specimens, a proximity ligation assay was used for dual detection of IR/IGF-IR hybrid receptor using both anti-IR and anti-IGF-IR antibodies. The PLA assay was optimized in both cell pellet and breast tissue specimens to detect IR/IGF-IR hybrid receptors. The presence of PLA signals was increased in cells had IR or IGF-IR overexpression and decreased in cells with IGF-IR knock down. The variability of signals was also observed in a tissue microarray with normal breast tissue and breast tumor.

15. SUBJECT TERMS
Insulin Receptor (IR), IGF-IR, IR/IGF-IR Hybrid receptor (Hybrid-R), inducible dimerization, Proximity ligation assay (PLA), breast cancer

16. SECURITY CLASSIFICATION OF:			**17. LIMITATION OF ABSTRACT**	**18. NUMBER**	**19a. NAME OF RESPONSIBLE PERSON**
a. REPORT	**b. ABSTRACT**	**c. THIS PAGE**			USAMRMC
U	U	U	UU	22	**19b. TELEPHONE NUMBER** *(include area code)*

Standard Form 298 (Rev. 8-98)

Table of Contents

Page

INTRODUCTION

Insulin receptor (IR) mediates the endocrine actions of insulin to regulate glucose homeostasis and metabolism [1]. The IGF signaling cascade is a major regulator of cell proliferation and survival, and thus it is important in many cancers including breast cancer [2-5]. IR/IGF-IR hybrid receptors (Hybrid-R) have been shown to occur when IR and IGF-IR are co-expressed[6]. Moreover, Hybrid-Rs are widely overexpressed in breast cancer specimens compared to normal breast tissue and the Hybrid-R levels are higher than both IR and IGF-IR levels in most breast cancer specimens[7]. However, Hybrid-R signaling and role of Hybrid-R in breast cancer remain un-known due to the difficulty to study the Hybrid-R specifically since they co-exist with IR and IGF-IR. **I hypothesize that Hybrid-Rs play a role in tumor progression by promoting cell proliferation, survival and migration, and that the levels of Hybrid-R may correlate with clinical outcome and biological characteristics of breast cancer patients.** In this study, I will utilize an inducible dimerization system to identify signaling pathways driven by Hybrid-R and develop a new assay that allows us to measure Hybrid-R levels on paraffin embedded specimens then further evaluate the prognostic value of Hybrid-R in breast cancer.

Body

1) Training environment

The Breast Center at BCM is an excellent teaching environment for graduate students and post-docs. In the past year, I have accomplished the following:

-Attended and presented data in poster format at San Antonio Breast Cancer Symposium (SABC) in San Antonio, TX, 2009

- Attended American Association of Cancer Research Annual Meeting (AACR) in Washington D.C., 2010

- Attended and presented data in poster format at TBMM Research Conference at Houston Marriott Hotel, Houston, TX, 2010

- Oral presentation at TBMM research seminar in Houston, TX, 2010

- Attended and presented data in poster format at Graduate School Symposium, at BCM, Houston, TX, 2010

2) Research Project

In this project, we are utilizing an inducible dimerization system in collaboration with Dr. Muthuswamy from Cold Spring Harbor to generate chimeric IR and chimeric IGF-IR to specifically study Hybrid-R. Chimeric IGF-IR retroviral vector with FKBP domain (IGF-IR-Fv2) and empty vectors with FKBP and FRB domain were provided by Dr. Muthuswamy. Homodimerizer AP20187 is used to dimerize chimeric IR with FKBP domain (IR-Fv2) or IGF-IR-Fv2 and heterodimerizer AP21967 is used to dimerize IGF-IR-Fv2 and chimeric IR with FRB (IR-FRB) to form Hybrid-R. The principle of inducible dimerization system for this project is attached in the Appendix I.

<u>Specific Aim 1:</u> Create breast cancer cell lines stably transfected with inducible receptors and identify signaling pathways and specific adaptor proteins activated by these inducible receptors.

- ***Construct retroviral vectors and confirm the expression for chimeric IR and chimeric IGF-IR protein expression***

To construct IR-Fv2 that allows homodimerization, the beta sub-unit of IR was PCR amplified and then inserted into retroviral empty vector with FKBP domain using XbaI enzyme. The same strategy was used to create IR-FRB that allows heterodimerization with IGF-IR-Fv2.

IGF-IRFv2 vectors were transfected into retrovirus packaging cell line PT67 and cells were harvested after antibiotic selection for stable expression of chimeric IGF-IR. As shown in Fig.1A, chimeric IGF-IR proteins were detected using both IGF-IR and HA antibodies and they have higher molecular weight than endogenous IGF-IR proteins.

IR-Fv2 and IR-FRB vectors were transiently transfected into 293 cells and cells were harvested at 48 hours after transfection for immunoblot analysis. In Fig. 1B, the IR-Fv2 was detected using both IR and HA antibodies and the IR-FRB was detected using both IR and Glu-Glu antibodies. Both kind of chimeric IR ran at higher molecular weight than endogenous IR.

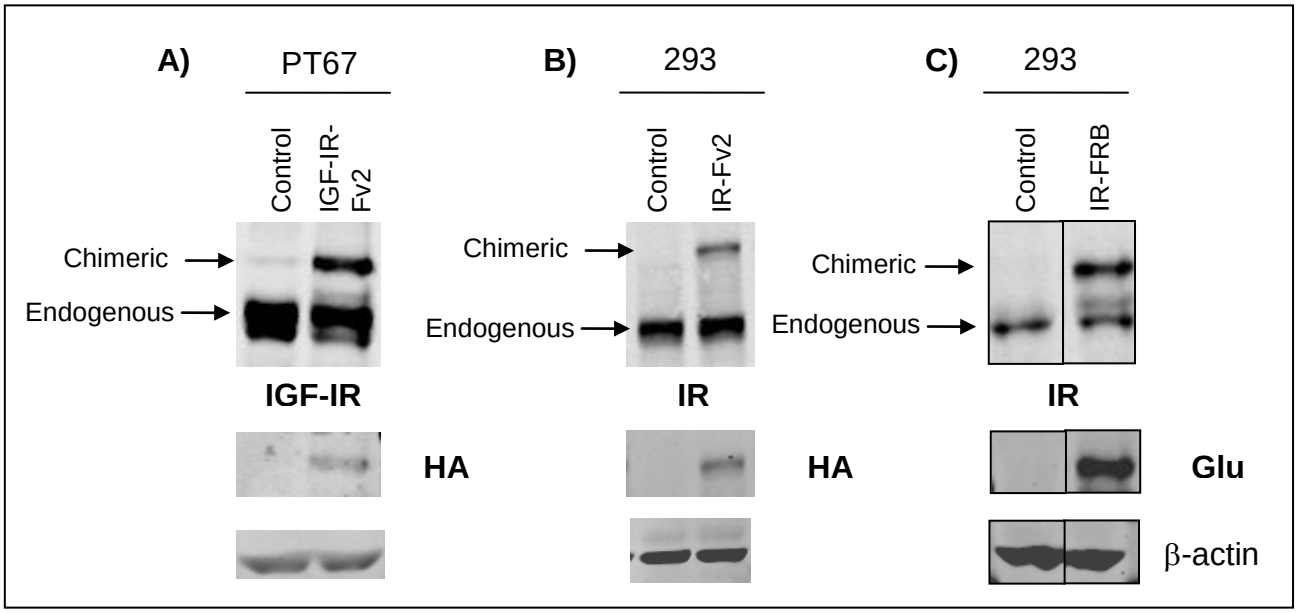

Figure 1. Expression of chimeric IR and IGF-IR in transiently transfected 293 and PT67 cells. A) Transfected PT67 cells were harvested after antibiotic selection for stable expression of chimeric IGF-IR. Proteins were harvested in 5% SDS buffer and analyzed by western blot for chimeric IGF-IR expression using anti-IGF-IR and anti-HA antibodies. B) and C) 293 cells were transiently transfected with chimeric IR with FKBP (IR-Fv2) or FRB domain (IR-FRB). Proteins were harvested at 48 hours after transfection for western blot analysis. Anti-IR and anti-HA antibodies were used to detect IR-Fv2 and anti-IR and anti-Glu-Glu antibodies were used to detect chimeric IR-FRB.

- ***Establishing MCF10A cells expressing chimeric IR and/or chimeric IGF-IR and their response to dimerizers***

Retroviruses for IGF-IR-Fv2 and IR-Fv2 were harvested from transient transfected PT67 cells for infection. Infected MCF10A cells were then subjected to 500ug/ml Geneticin selection. Geneticin resistant clones were harvested for immunoblot to confirm the IGF-IR-Fv2 or IR-Fv2 expression. I have generated two stable MCF10A pools: IGF-IR-Fv2 and IR-Fv2 by pooling all positive stable clones after screening. Prior to establishing stable MCF10A clones for IR-Fv2, I performed immunoblot analysis on MCF10A IGF-IR-Fv2 pools treated with or without homodimerizer AP20187 to verify the functionality of IGF-IR-Fv2 (Fig. 2). As expected, treatment of AP20187 successfully induced phosphorylation of chimeric IGF-IR and activation of AKT and ERK. Interestingly, phosphorylation of IGF-IR-Fv2 and AKT seemed

to be saturated at the lowest dose (20nM) in this experiment. This suggested that a lower dose range should be used to further characterize the dose response of IR-Fv2 and IGF-IR-Fv2.

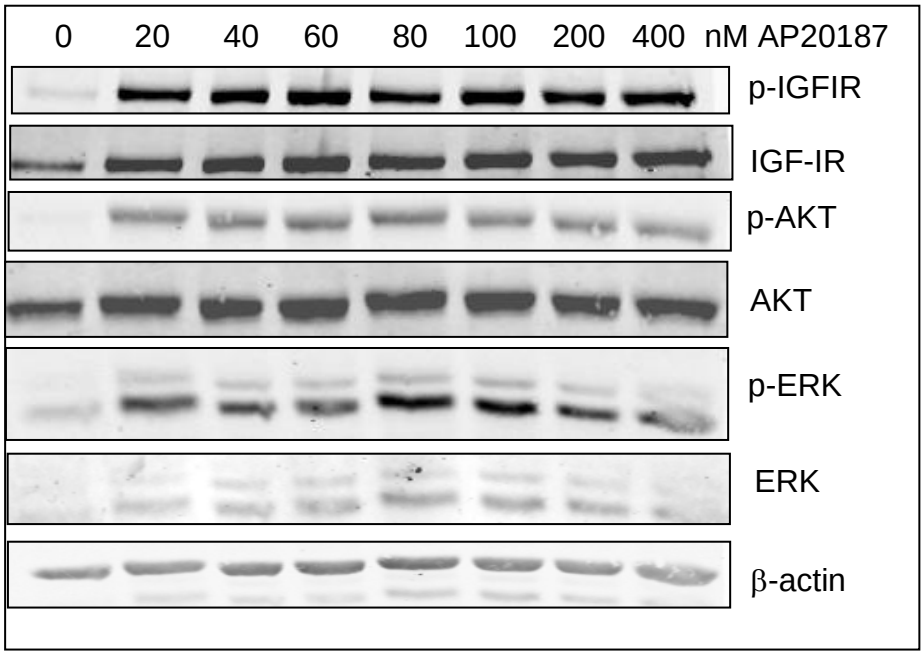

Figure 2. AP20187 induces activation of IGF-IR-Fv2 and down stream AKT and ERK in MCF10A cells. MCF10A cells stably expressing IGF-IR-Fv2 were treated with incremental doses of AP20187 for 15 minutes after serum free medium (SFM) starvation overnight. Proteins were detected by western blot using antibodies against p-IGFIR, IGF-IR, p-AKT, AKT, p-ERK, ERK and β-actin.

After established stable clones for IR-Fv2, I used another dose range of AP20187 to test the functionality of IR-Fv2 in comparison of IGF-IR-Fv2. We found that AP20187 was able to induce both IR-Fv2 and IGF-IR-Fv2 activation and increase of AKT and ERK phosphorylation in a dose dependant manner (Fig 3). However, the magnitude of chimeric receptor and AKT activation in MCF10A IR-FV2 pool was much smaller compared to IGF-IR-Fv2 pool. From the HA blot that detect the levels of IR-Fv2 and IGF-IR-Fv2, it seems like the expression levels of transgene was much less in IR-Fv2 pool compared to IGF-IR-Fv2 pool. I performed an immunoblot to compare the HA levels in all IR-Fv2 and IGF-IR-Fv2 individual clones and found that 3 out of 4 IR-Fv2 clones had much less levels of transgene expression compared to IGF-IR-Fv2 clones (data not shown). Low levels of transgene expression could be one of the reasons that the same dose of AP20187 wasn't able to induce the same levels of response in IR-FV2 cells. In addition, stable IR-Fv2 cells had longer doubling time and were not as health as stable IGF-IR-Fv2 cells as they produced much more debris in culture medium. It was hard to rule out if it's because of position of the transgene incorporated into the genome or in the process of antibiotic selection that led to this difference between stable IR-Fv2 and IGF-IR-Fv2 cells. Therefore, we will try to re-establish another set of stable clones for IR-Fv2.

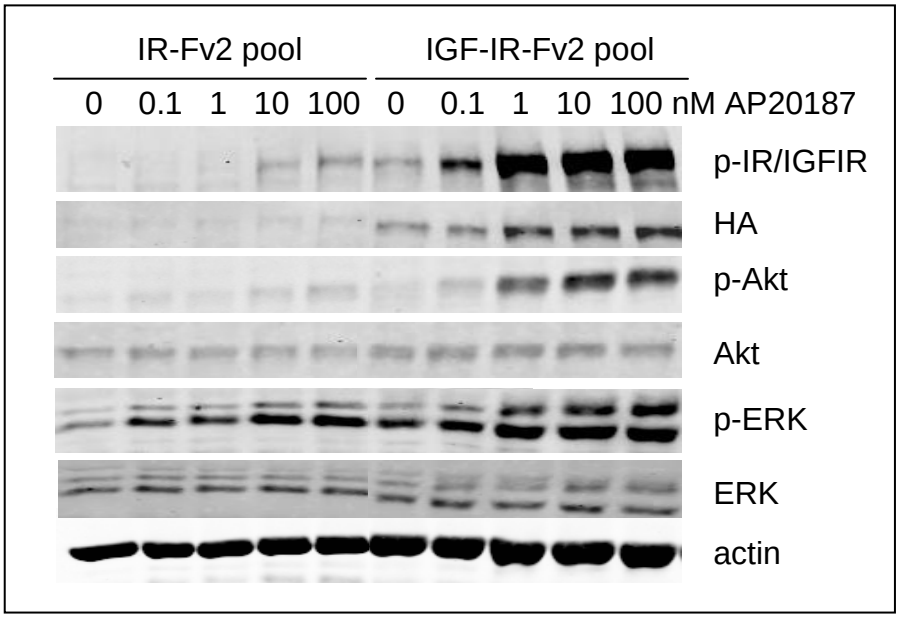

Figure 3. AP20187 induces activation of IR-Fv2 and IGF-IR-Fv2 and down stream AKT and ERK in MCF10A cells. MCF10A IR-FV2 pool and IGF-IR-Fv2 pool were generated by pooling all positive clones with 1 to 1 ratio. Cells were starved in SFM overnight then treated with incremental doses of AP20187 for 15 minutes. Protein levels were detected by western blot using antibodies against p-IR/IGF-IR, HA, p-Akt, Akt, p-ERK, ERK and β-actin.

We also established 3 stable MCF10A clones expressing IR-FRB (data not shown). In order to create cells expressing both IR-FRB and IGF-IR-Fv2 that allow us to induce IR/IGF-IR Hybrid formation specifically, we had transfected them with IGF-IR-Fv2. Transfected cells were put under both 500ug/ml Geneticin and 5ug/ml Puromycin selection to select for double positive cells. However, we had tried two sets of transfection and wasn't able to establish stable clones in the process of clone expansion. We planed to try another transfection reagent to improve the transfection efficiency and perform the selection again.

<u>Specific Aim 2:</u> Investigate phenotypic changes in breast cancer cells expressing IR/IGF-IR hybrid receptor and identify signaling pathways that lead to these phenotypic changes.

Not yet started. We proposed to perform study if activation of IR/IGF-IR Hybrid could promote cell proliferation or migration in MCF10A cells. However, we weren't able to establish stable cell lines expression both IGF-IR-Fv2 and IR-FRB allowing us to continue the study. Since IR/IGF-IR hybrid binds to both insulin and IGF, it would be important to understand how different breast cell lines respond to insulin and IGF stimulation. Therefore, we initiated a comparative study for insulin and IGF action using a panel of breast cancer cell lines. In this study, we compare gene expression of insulin and IGF system as well as multiplex proteomic profiling using reverse phase protein array (RPPA) to compare the characteristics and the relationship to insulin and IGF response in different breast cancer cell lines. From this study, we could gain understanding of insulin and IGF signaling and then select better candidate cell lines as model for future studies. The progress of this study will be listed after aim 3.

<u>Specific Aim 3:</u> Determine the levels of IR/IGF-IR hybrid receptors in breast cancer samples and correlate these to clinical characteristics and outcome.

In the proposal, I proposed to use FRET/FLIM technique to measure the Hybrid-R on paraffin embedded samples. However, I encountered some difficulties to find the microscope with FLIM capability and it is more difficult to quantify the lost of signal instead of gain of signal. Therefore, I decided to switch to proximity ligation assay (PLA) developed by Olink Bioscience to measure the Hybrid-R. The principle of PLA assay is attached in the Appendix II.

- ***Create control samples for PLA assay development***

I generated cell pellet controls using transient transfection of IR or IGF-IR in 293 cells and siRNA knock down IGF-IR in MDA-MB-134 to create samples with different levels of Hybrid-R expression. Transfected cells were harvested on parallel for cell lysate and paraffin embedded blocks. From immunoblot and immunohistochemistry (IHC) of IGF-IR (Fig. 4A-C), we observed significant decrease of signal on IGF-IR siRNA transfected MDA-MB-134 cells and increase of signal on IGF-IR transfected 293T cells. In addition, increase of IR expression was also confirmed in IR transfect 293T cells (Fig. 4C-D).

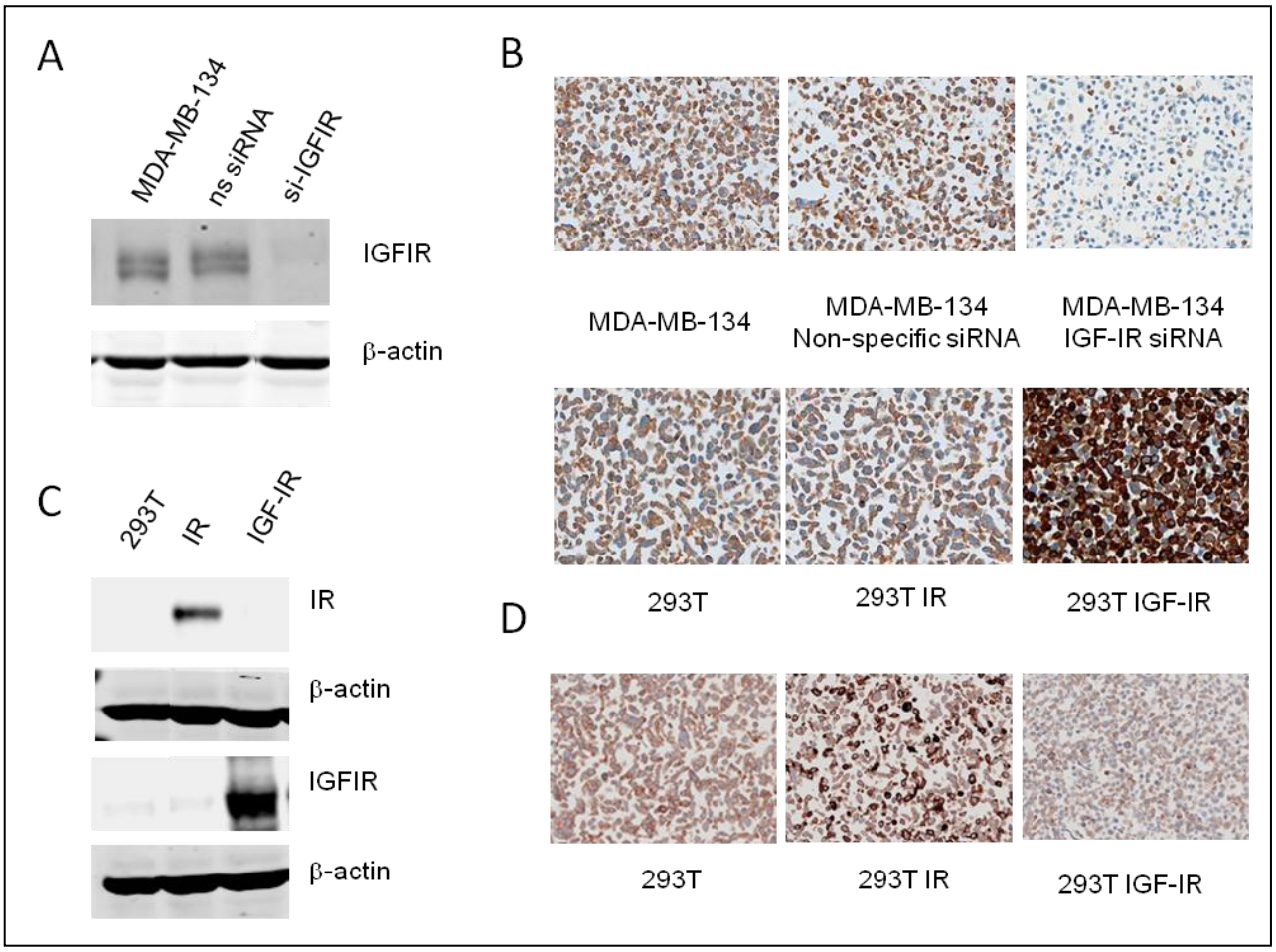

Figure 4. Immunoblot and IHC for IR and IGF-IR in transfected MDA-MB-134 and 293T cells. MDA-MB-134 cells were transiently transfected with non-specific siRNA or IGF-IR siRNA. 293T cells were transiently transfected with IR or IGF-IR. Cells were scraped down and lysed in 5% SDS for immunoblot or fixed in 10% formalin for two hours prior embedding into paraffin block. Protein levels were detected by western blot using antibodies against IGF-IR, IR and β -actin. A. Decrease of IGF-IR expression in IGF-IR siRNA transfected MDA-MB-134 cells. B. Immunoblot confirmed the increase of IR and IGF-IR expression in IR and IGF-IR transfected 293T cells respectively. C. IGF-IR IHC on MDA-MB-134 and 293T cell pellets. D. IR IHC on 293T cell pellets.

- ***Optimization of PLA assay for Hybrid-R detection***

To test if the antibody pair could be used for Hybrid-R detection in PLA assay, I used sections from MDA-MB-134 cell pellets to perform the PLA assay. In this experiment, I included several technical negative controls to confirm that the signal is truly from the dual recognition of IR and IGF-IR antibody to the Hybrid-R, not from non-specific binding of probes or IR antibody or IGF-IR antibody alone. As shown in figure 5, there was no signal detected on no antibody control, no IR antibody and no IGF-IR antibody control. In contrast, there were bright red spots (indicated by white arrow in

fig. 5 detected on MDA-MB-134 sections while the signal was absent in MDA-MB-134 section with IGF-IR siRNA knock down.

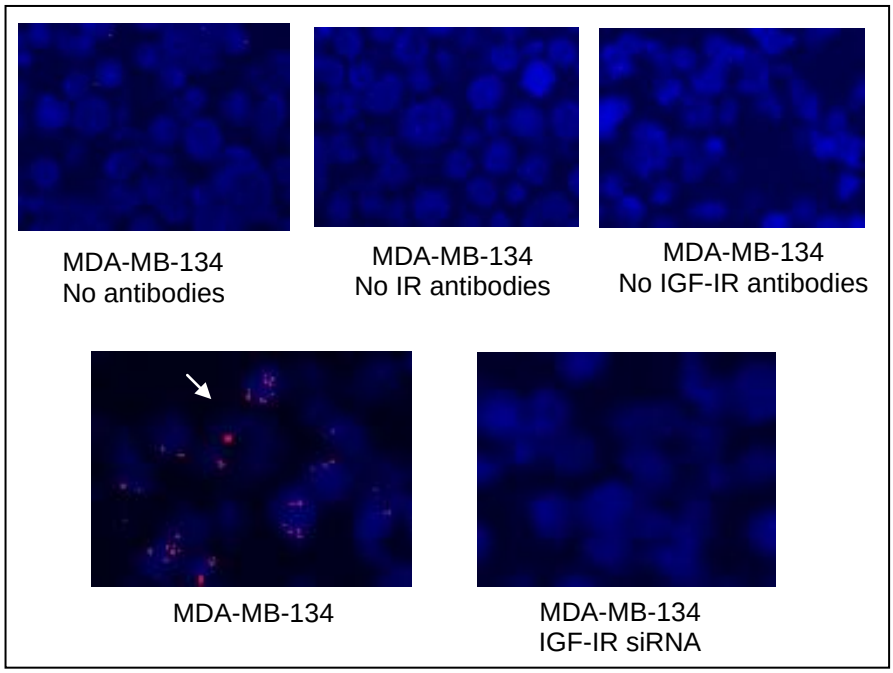

Figure 5. Detection of Hybrid-R on MDA-MB-134 cell pellet samples using PLA assay. MDA-MB-134 cell pellet sections were deparaffinized in Xylene. They were then placed in sodium citrate buffer and cooked for 20 minutes in pressure cooker for antigen retrieval. Blocking buffer provided in the PLA assay kit was used for blocking for 30 minutes. Monoclonal anti-IR antibody from Santa Cruz and Polyclonal anti-IGF-IR antibody from Cell Signaling were used as primary antibody pair for duo recognition of Hybrid-R. The rest of the processes were performed according to the instruction from the PLA assay manual. The images were taken by Nuance system, a multispectral image system developed by CRI

I then performed another PLA assay on tissue microarray (TMA) that contains transfected cell pellet samples with different levels of IR or IGF-IR expression. In accord with the observation from the last experiment, the signal was decreased in IGF-IR siRNA transfected compared to non-specific siRNA transfected MDA-MB-134 cells. In addition, there was increased of signals in IR or IGF-IR transfected 293T cells compared to non-transfected control. (Fig. 6)

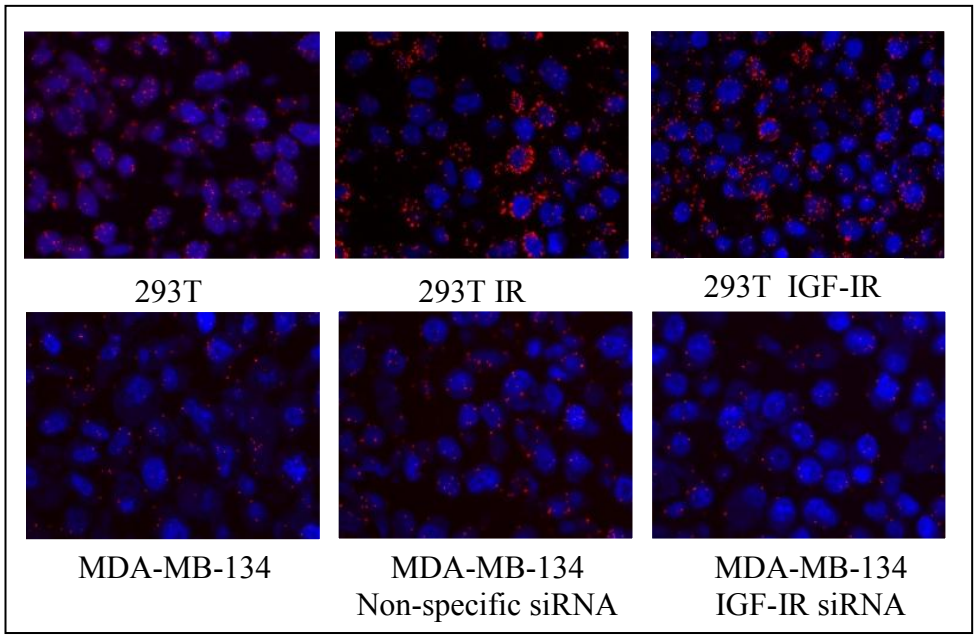

.**Figure 6. Difference of IR/IGF-IR Hybrid signals detected by PLA in transient transfected 293T and MDA-MB-134 cells.** Cell pellets with different

levels of IR and IGF-IR expression were made into a tissue microarray and 5μm sections were made for staining. Sections were deparaffinized and subjected to antigen retrieval as previously described. The blocking and primary antibody condition in previously experiment was followed and the rest of the processes were performed according to the instruction from the PLA assay manual. The images were taken by Nuance system, a multispectral image system developed by CRI

Next, I performed a PLA assay on a TMA slides with normal breast tissue and dead-end breast tumors to determine if the condition for cell pellet controls could also work on tissue samples. As shown in figure 7, the signal (indicated as white arrow) was present in some but not all tissue samples. However, it was difficult to visualize and quantify the staining signals in tissue samples due to the high fluorescence background.

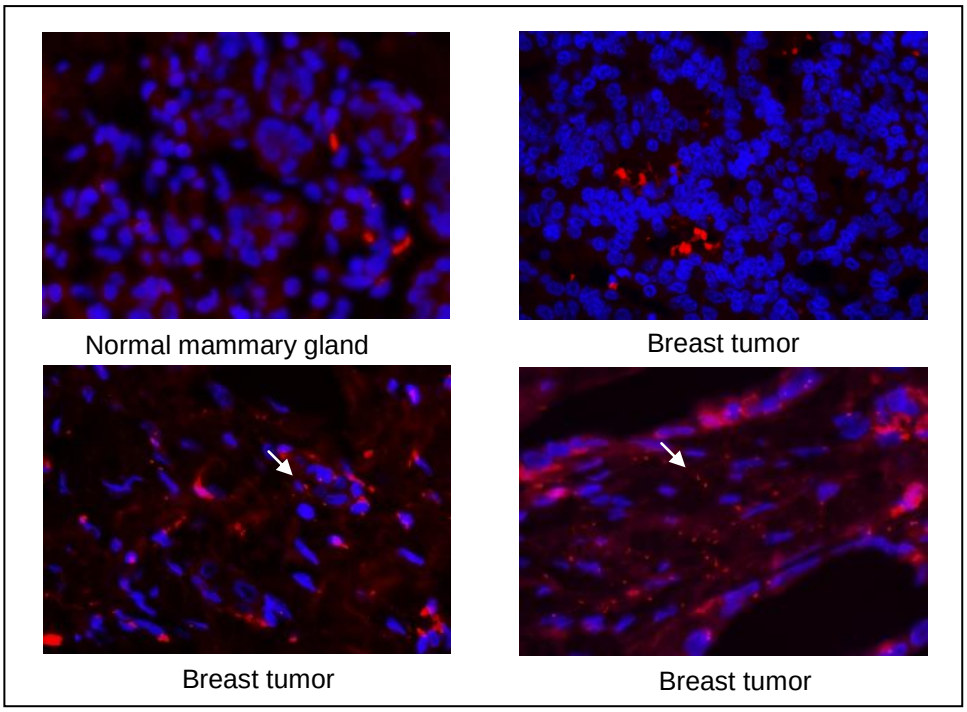

Figure 7. Detection dead end breast tissue samples using PLA assay. A TMA slide with dead-end normal breast tissue and breast tumor specimens from Breast Center pathology core was used to test the PLA assay on tissue specimens. The staining condition used for cell pellet samples was followed in this assay and the images were also acquired using Nuance system.

I have encountered some technical difficulties in reducing the fluorescence background in this fluorescence based PLA assay. Therefore, I also tried to the newly developed HRP-based PLA assay that would allow us to exam the staining result under bright field microscope. I am currently in the process of identifying optimal condition for signal amplification on positive controls provided by the company.

Comparative transcriptional and proteomic profiling of insulin and IGF action in a large panel of breast cancer cell lines.

Breast cancer is a very heterogeneous disease and could be divided into subtypes based on clinical and molecular characteristics of tumors. Molecular analysis have been conducted on a collection of breast cancer cell lines in

comparison with breast tumors suggesting that they could be used as models to study distinct subtypes of breast cancer [8]. To investigate if there is a potential correlation of insulin and IGF activities to specific breast cancer subtype, we decided to perform a serious of gene expression and protein profiling analysis in a panel of 21 breast cancer cell lines in our laboratory. Gene expression profile data from Neve *et. al*, 2006 was used in clustering analysis to compare insulin and IGF axis gene between different subtypes of breast cancer cell lines [8]. Hierarchical clustering analysis on combination of ligands, receptors, IRSs and IGFBPs probe subsets was performed and Basal B cell lines and PR positive cell lines were identified as distinct clusters. As shown in figure 8, luminal cell lines seem to be associated with higher insulin and IGF-I and IGF-II compared to basal A and basal B cell lines. Basal B cell lines seem to associate with higher IRS2 as well as IGFBP6 and IGFBP7 expression. In addition, analysis on subsets of probes was performed and ER positive cell lines were associated with higher IGFBP2, 4 and 5 (data not shown).

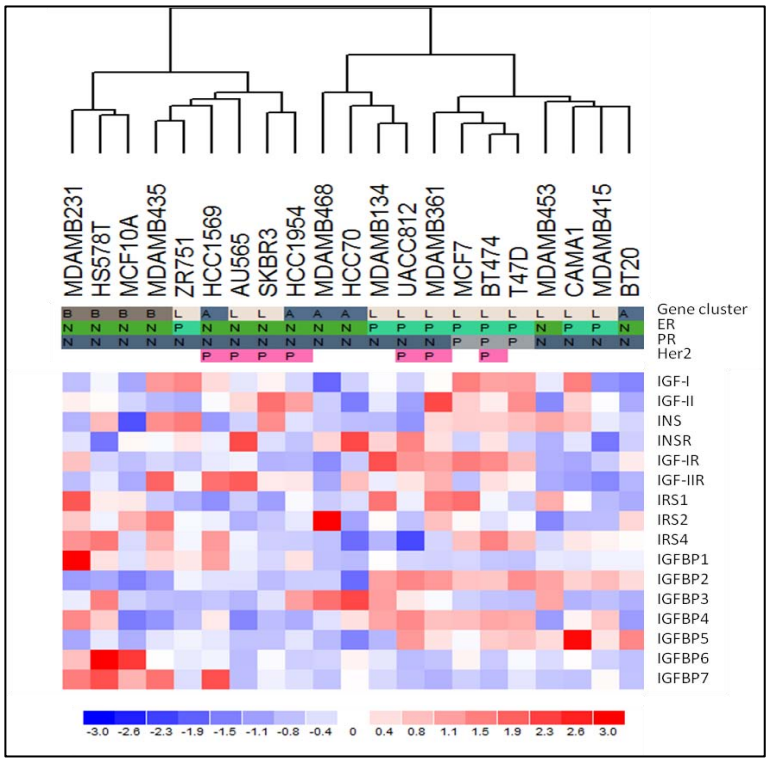

Figure 8. Insulin and IGF axis expression profile of 21 human breast cancer cell lines. Gene expression data from Neve et, al 2006 was used to compare markers insulin and IGF axis expression. Hierarchical clustering analysis was performed using probes for IGF-I, IGF-I, INS, IR, IGF-IR, IGF-IIR, IRS1-4 and IGFBP1-7 on dCHIP software. Gene expression levels are presented by log2 pseudo-color scale.

We then measured IR and IGF-IR mRNA as well as protein levels in the same panel of breast cancer cell lines and compare that to the gene expression analysis result. As shown in figure 9, IGF-IR and IR receptor levels are very variable and no obvious association between IR and IGF-IR level to specific subtypes of breast cancer cells was observed. However, high IR levels in MDA-MB-468 and ZR-75-1 and high IGF-IR levels in MCF7 and MDA-MB-134 were generally in accord with the finding from Q-RT-PCR and RPPA (Figure 9).

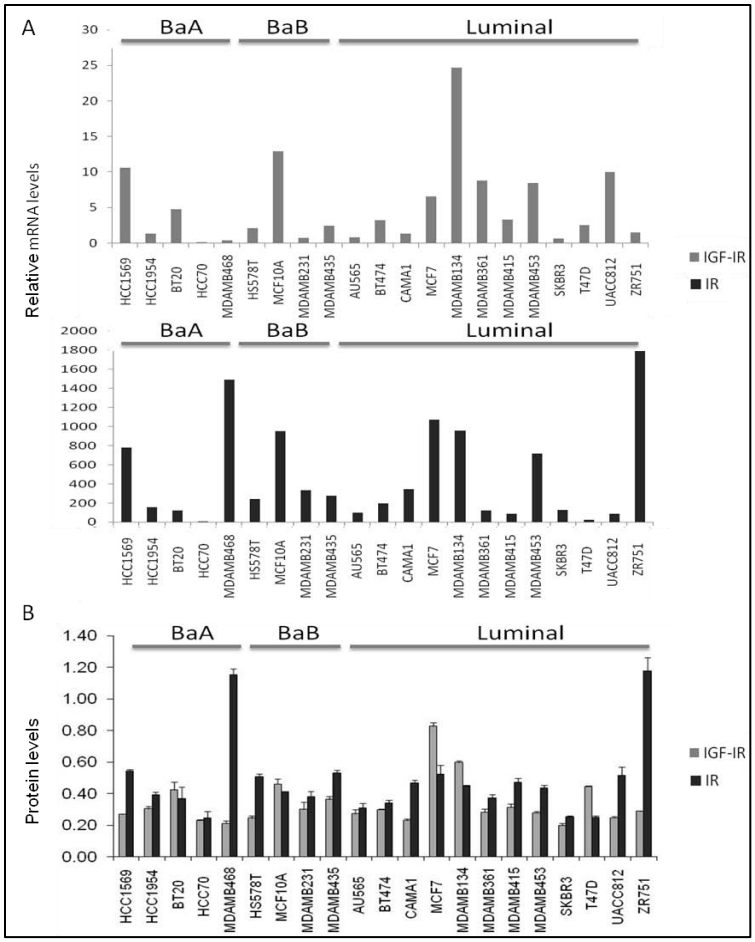

Figure 9. IR and IGF-IR mRNA and protein in breast cancer cell lines measured by Q-RT-PCR and RPPA. A. Cell lines under normal culture condition were harvested and 1ug of mRNA were extracted and converted to cDNA via RT reaction. IR measured by SYBR and IGF-IR by Taqman qPCR on 5ul of cDNA. B-actin was measured as control for gene expression normalization and $\Delta\Delta$CT method relative quantification was used for comparison of relative fold of IR and IGF-IR expression in different cell lines. Cell lines were arranged by gene clustered subtypes based on their transcriptional profile. B. Cells were cultured in triplicate were harvested in RPPA lysis buffer. IR and IGF-IR protein levels were measured by RPPA and values from non treated control to compare receptor levels in this panel of breast cancer cell lines. Cell lines were arranged by gene clustered subtypes based on their transcriptional profile.

In order to gain better understanding the action of insulin and IGF in breast cancer, our lab utilized Reverse Phase Protein Array (RPPA) to study insulin and IGF induced protein profile in 21 different breast cancer cell lines in collaboration with Department of Systems Biology in MD Anderson. In this study, we stimulated 21 breast cancer cell lines with either insulin or IGF at 10nM for six different time points (5, 10, 30 minutes, 6, 24 and 48 hours) in triplicate and profiled 134 different phospho-protein and non-phospho protein markers that involved in growth factor signaling pathways as well as cell cycle regulation and DNA repair.

In order to identify effects induced by insulin and IGF, we used serum free non-treated control as baseline to determine the fold change of protein levels induced by insulin or IGF. In preliminary analysis, we selected protein changed for greater than 1.3 or -1.3 fold to generate insulin and IGF profile for each cell line and use dCHIP software for clustering analysis to compare them among different cell lines. As shown in figure 10, insulin and IGF induced similar protein profile within each cell line. However, there were differences of profile patterns within and between cell lines. Among these 21 cell lines, we identified several basal B

(MCF10A, MDA-MB-231 and MDA-MB-435) and luminal (MCF7, ZR-75-1, T47D, MDA-MB-134, and MDA-MB-415 and MDA-MB-453) cell lines with increase of markers activation in PI3K pathway upon IGF or insulin stimulation.

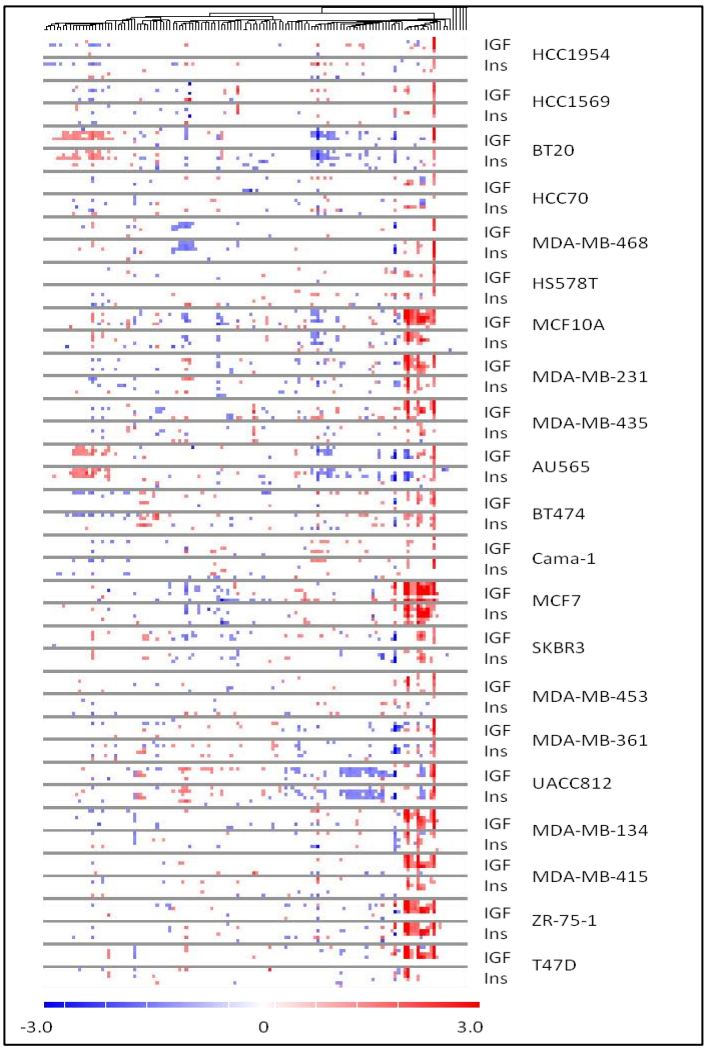

Figure 10. Clustering of insulin and IGF induced protein changes in 21 breast cancer cell lines. Thumbnail heatmap of clustering analysis of protein fold change induced by insulin and IGF throughout 6 different time points in 21 cell lines. Values from triplicate were averaged and serum free non treated controls were used as baseline for normalization and for relative protein fold change calculation. One-way ANOVA with contrast was performed to identify proteins that are statistically significantly modulated by insulin and IGF. In this analysis, protein fold changes greater than 1.3 fold (in red), less than -1.3 fold (in blue) were included in hierarchical analysis and depicted by log 2 pseudo-color scale shown (fold changes between 1.3 and -1.3 or non statistical significant were shown in blank). Protein fold changes within IGF or Insulin (Ins) row for each time point were presented in longitudinal order: 5, 10, 30 minutes, 6, 24 and 48 hours.

From this analysis, we found that majority of proteins with significant changes disappear at 24 and 48 hour time points and patterns from 10 minutes to 6 hour time points are generally consistent. We then performed hierarchical clustering analysis on results from 30 minutes time point and to identify cell lines with similar insulin and IGF response. As shown in figure 11, we found 2 groups of cells with distinct pattern. One group of cell lines clustered with MCF7 including both basal B and luminal cells and there seems to be no obvious correlation between ER status and the response to insulin or IGF. In this cluster, insulin or IGF treatment significantly induced AKT, S6K, p70S6K and STAT5 phosphorylation. Moreover, results of insulin and IGF treatment clustered tightly together in MCF7, MCF10A and ZR-75-1 cells. We then took a closer look at the

insulin and IGF induced fold changes in these cell lines and found that IGF is more potent activator compared to insulin. For example, IGF induced more than 10 fold of AKT phosphorylation in contrast to 5 and 3 fold activation induced by insulin in MCF7 and MCF10A cells. However, ZR-75-1 cells which have significant high IR expression, insulin and IGF induced comparable fold AKT and MAPK phosphorylation. In addition, we found a group of cell lines had significant decrease of p-MAPK upon insulin or IGF stimulation including AU565, BT-20, UACC812, MDA-MB361, SKBR3, BT474 and MDA-MB-468. Interesting, majority of them are Her2 positive cell lines except MDA-MB-468 which has EGFR overexpression suggesting insulin and IGF may play role in negative feedback mechanism in cell lines with other growth factor pathway activation. In the future, we are interested in comparing the effect of insulin and IGF in cell proliferation in cell lines that clustered with MCF7 and identifying mechanism for insulin and IGF induced MAPK de-phosphorylation in Her2 positive cell lines.

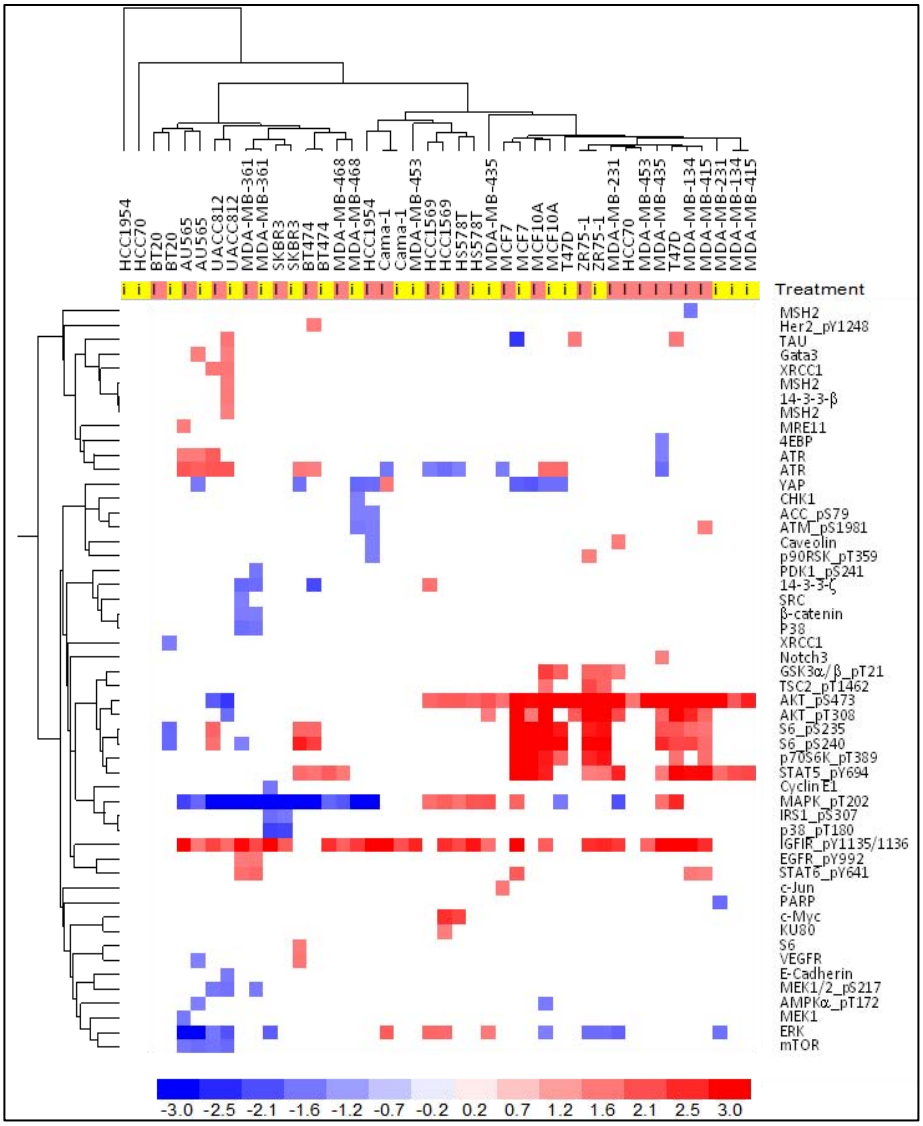

Figure 11. Clustering analysis of insulin and IGF protein identified 2 groups of cell lines with distinct response.

Two way hierarchical clustering analysis of protein changed induced by 30 minutes of insulin or IGF treatment was perfomed. One-way ANOVA with contrast was performed to identify proteins that are statistically significantly modulated by insulin and IGF. In this analysis, protein fold changes greater than 1.5 fold (in red), less than -1.5 fold (in blue) were included in hierarchical analysis and depicted by log 2 pseudo-color scale shown (fold changes between 1.5

and -1.5 or non statistical significant were shown in blank). Insulin treament was coded in yellow and IGF treatment was coded in pick in dendrogram annotation.

Key Research Accomplishments

- Confirmed the expression and functionality of IGF-IR-Fv2 in MCF10A cells.
- Constructed retroviral vector for IR-Fv2 and IR-FRB and confirmed the expression of chimeric IR with FKBP and chimeric IR with FRB in transiently transfected 293 cells.
- Established stable MCF10A clones for IR-Fv2 and IR-FRB.
- Optimized PLA assay for IR/IGF-IR Hybrid receptor detection in paraffin embedded specimens.
- Preliminary analysis of insulin and IGF induced protein changes in 21 breast cancer cell lines.

Reportable Outcomes

Gualberto A, Filhart MD, Gustavson M, Christiansen J, **Wang Y**, Hixon ML, Reynolds J, McDonald S, Panjikaran M, Rimm DL, Langer CJ, Blakely J, Garland L, Paz-Ares LG, Karp DD, Lee AV. Molecular analysis of non-small cell lung cancer identifies tumor subsets with differential sensitivity to insulin-like growth factor receptor inhibition by figitumumab. *Clinical Cancer Research.* 2010 Sep 15;16(18):4654-4665

Conclusion

It has been very difficult to specifically study the role of IR/IGF-IR Hybrid receptor (Hybrid-R) since it is impossible to stimulate endogenous Hybrid-R without activating IR or IGF-IR. Therefore we proposed to utilize inducible dimerization system to differentiate the effect of Hybrid-R from that of IR and IGF-IR. Unfortunately, we are having technical difficulties in creating stable IR-Fv2 clones and double positive clones for IR-FRB+ IGFIR-Fv2 in immortalized epithelial cell lines MCF10A. As working on inducible chimeric receptor system, we realized that more studies are needed to compare the insulin and IGF responses in different breast cancer cells. Therefore, we embarked on a study to compare the gene expression profile and insulin and IGF induced protein changes in a panel 21 breast cancer cell lines. From this study, we could also gain more insights about selecting suitable cell line models for studying the function of Hyrbrid-R.

The objective of developing PLA assay is to allow us to have a better way to measure and quantify IR/IGF-IR Hybrid in archived breast tumor samples that are mostly in paraffin embedded format and determine if levels of IR/IGF-IR hybrid could have any prognostic significance for breast cancer. The preliminary result of PLA assay on cell pellet samples was promising and we did observed difference of signal in a set of breast tissue samples. However, the high fluorescence background makes it technically challenging to quantify the signals. I hope I could resolve this issue either by optimizing auto-fluorescence quenching on paraffin embedded tissues or optimizing HRP-based PLA assay.

IGF-IR activation is known to be important in many aspects of tumor progression and therapeutic agents are developed to target IGF-IR. There are 2 main categories of IGF-IR therapeutic agents: anti-IGF-IR antibody that is specific to IGF-IR and tyrosine kinase inhibitor (TKI) that inhibit both IR and IGF-IR. Oral administer of TKI is easier than infusion of monoclonal antibody into patients but inhibit insulin signaling will be more toxic to patients. However, insulin signaling activation could be one resistant mechanism to anti-IGFIR antibody therapy due to the high homology of these two pathways. From the preliminary analysis of the RPPA result we have identified cell lines are responsive to both insulin or IGF stimulation and they could further be used as candidate cell lines to study insulin action and their relationship to anti-IGF-IR therapy.

Due to the technical difficulty we encountered in studying the IR/IGF-IR Hybrid project, that I becoming more senior in my graduate study and we have many interesting finding from the RPPA project, my mentor Dr. Adrian Lee and I decided to mainly focus on the RPPA project in the remaining time of my graduate training. Therefore, I would include the reportable finding of this RPPA project as my final report.

References

1. Dupont, J. and D. LeRoith, *Insulin and insulin-like growth factor I receptors: similarities and differences in signal transduction.* Horm Res, 2001. **55 Suppl 2**: p. 22-6.
2. Sachdev, D. and D. Yee, *The IGF system and breast cancer.* Endocr Relat Cancer, 2001. **8**(3): p. 197-209.
3. LeRoith, D. and C.T. Roberts, Jr., *The insulin-like growth factor system and cancer.* Cancer Lett, 2003. **195**(2): p. 127-37.
4. Zhang, D., A.A. Samani, and P. Brodt, *The role of the IGF-I receptor in the regulation of matrix metalloproteinases, tumor invasion and metastasis.* Horm Metab Res, 2003. **35**(11-12): p. 802-8.
5. Samani, A.A., et al., *The role of the IGF system in cancer growth and metastasis: overview and recent insights.* Endocr Rev, 2007. **28**(1): p. 20-47.
6. Maria A. Soos, J.W., Reiner Lammers, Axel Ullrich, and Kenneth Siddles, *Receptors for insulin and insulin-like growth factor-I can form hybrid dimers.* Biochem. J., 1990. **270**: p. 383-390.
7. Francesco Frasca, G.P., Riccardo Vigneri, and Ira D.. Goldfine, *Insulin and hybrid insulin/IGF receptors are major regulators of breast cancer cells.* Breast Disease, 2003. **17**: p. 73-89.
8. Neve, R.M., et al., *A collection of breast cancer cell lines for the study of functionally distinct cancer subtypes.* Cancer Cell, 2006. **10**(6): p. 515-27.

Appendix

I. Inducible dimerization system

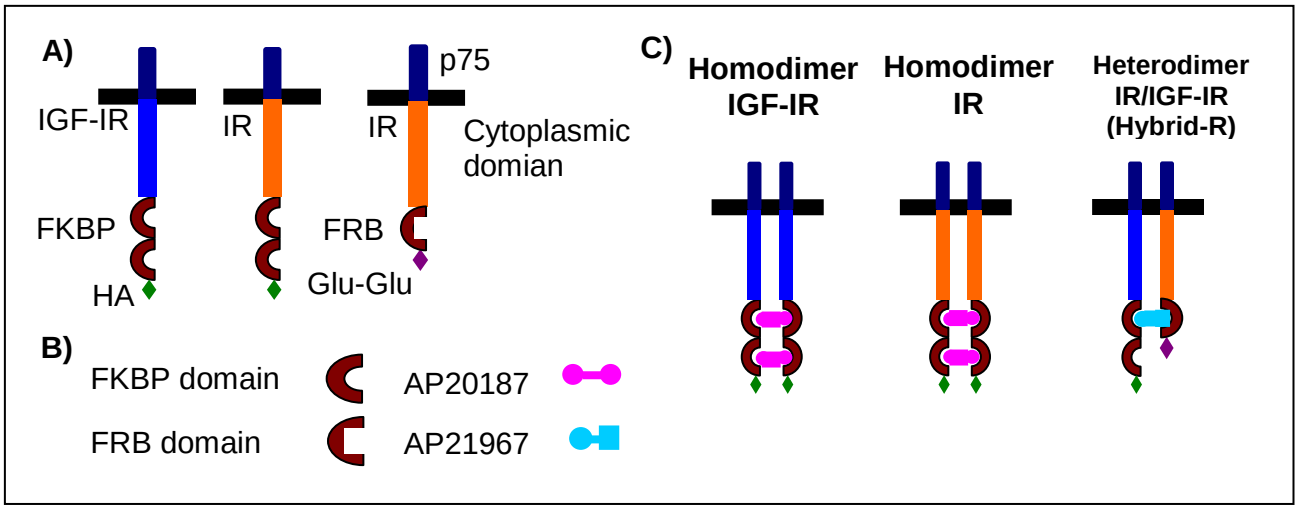

Each chimeric receptor consists of extra-cellular domain of p75 that avoids the ligand binding (insulin, IGF-I and IGF-II) to the chimeric receptor, beta sub-unit of IR or IGF-IR, dimerization domain (FKBP or FRB) and a tag (HA or Glu-Glu). There are three different chimeric receptors in this system: (1) Chimeric IGF-IR with FKBP domain (IGF-IR-Fv2) tagged with HA (2) Chimeric IR with FKBP domain (IR-Fv2) tagged with HA (3) Chimeric IR with FRB domain (IR-FRB) was tagged with Glu-Glu. There are two kinds of dimerizers: AP20187 that brings two FKBP domains together for homodimerization and AP21967 that brings one FKBP and one FRB domain together for heterodimerization.

II. Principle of PLA assay (from Duolink PLA manual by Olink Bioscience)

Typical starting materials are adherent cells, cytospin preparations or tissue sections on a glass slide, fixed, pre-treated and blocked with a blocking reagent according to the requirements of the primary antibodies used.

1: The samples are incubated with primary antibodies that bind to the protein(s) to be detected.

2: Secondary antibodies conjugated with oligonucleotides (PLA probe MINUS and PLA probe PLUS) are added to the reaction and incubated.

3: The Hybridization solution, consisting of two oligonucleotides (illustrated as red bands), is added and the oligonucleotides will hybridize to the two PLA probes if they are in close proximity.

4: The Ligation solution is added together with Ligase (yellow), joining the two hybridized oligonucleotides to a closed circle.

5: The Amplification solution, consisting of nucleotides (not shown) is added together with Polymerase (yellow). The oligonucleotide arm of one of the PLA probes acts as a primer for a rolling-circle amplification (RCA) reaction using the ligated circle as a template, generating a concatemeric (repeated sequence) product extending from the oligonucleotide arm of the PLA probe.

6: The Detection solution, consisting of fluorescently labeled oligonucleotides, is added and the labeled oligonucleotides will hybridize to the RCA product. The signal is easily visible as a distinct fluorescent dot and analyzed by fluorescence microscopy.